ISSN 1749-3889 (print), 1749-3897 (online)
International Journal of Nonlinear Science
Vol.17(2014) No.3,pp.241-253

Usage of Higher Order B-splines in Numerical Solution of Fisher's Equation

Ali Şahin *, Özlem Özmen
Department of Mathematics, Aksaray Univesity, 68100, Aksaray, Turkey.
(Received 3 October 2013, accepted 18 April 2014)

Abstract: In this paper, the collocation method is performed with quintic B-spline functions on a uniform mesh to obtain the numerical solutions of Fisher's equation. Crank-Nicolson method is used for time discretization. Von Neumann stability analysis shows that the given method is conditionally stable. In order to observe the effects of reaction and diffusion, four test problems related to pulse disturbance, step disturbance, super-speed wave and strong reaction are studied. A comparison between the obtained results and some earlier studies is presented.

Keywords: B-Spline, collocation, Fisher's equation, reaction-diffusion, Von Neumann

1 Introduction

Fisher's equation which was first appeared in Fisher's study [1] is one of the most famous nonlinear reaction-diffusion equation in the literature. The equation is given by

$$\frac{\partial u}{\partial t} = \mu \frac{\partial^2 u}{\partial x^2} + \rho u(1-u), \quad x \in (-\infty, \infty), \; t > 0 \tag{1}$$

where $u = u(x,t)$ is a real-valued function, μ is a non-negative constant and ρ is a real parameter. $\mu \partial^2 u/\partial x^2$ is called diffusivity term where $\rho u(1-u)$ describes the reaction of the system.

Fisher[1] used Eq.(1) to describe the propagation of gene in a habitat. The growth of the mutant gene population originates from the diffusion and nonlinear local multiplication. Because of the similar behavior, Eq.(1) is also used as a model for the evolution of the neutron population in a nuclear reactor where the domain is obviously finite [5].

The initial and boundary conditions for Fisher's equation are given as

$$u(x,0) = u_0(x) \in [0,1], \quad x \in (-\infty, \infty) \tag{2}$$

$$\lim_{x \to -\infty} u(x,t) = 1 \, , \lim_{x \to \infty} u(x,t) = 0, \quad t \geq 0 \tag{3}$$

$$\lim_{x \to \pm\infty} u(x,t) = 0 \, , t \geq 0 \tag{4}$$

where the x derivative tending to zero while $x \to \pm\infty$. In the literature, conditions (2) and (3) together are commonly known as nonlocal conditions, while conditions (2) and (4) together are usually known as local conditions [23]. One of the known numerical difficulty of Fisher's equation is the sensitivity of a correct solution especially at the right-hand boundary. Numerical methods may lead to erroneous results if they don't consider the sensitive solution that depends on the initial distribution at infinity [6, 12, 15, 19].

There are many theoretical and numerical studies on Fisher's equation in the literature. Kolmogorov *et al.*[2] showed that for every $c \geq 2$ there exists a travelling wave solution to (1)−(3) of wave speed c. Each of these solutions is bounded as $u_0(x)$ in Eq.(2) and there is no such solutions for $c \in [0,2)$. An important property in numerical solution of Fisher's equation is shown by Canosa[5] that stability of the solution to perturbations of compact support, whereas instability occurred when the perturbation vanished at infinity. Gazdag and Canosa[6] produced a numerical solution of Fisher's equation and demonstrated the mechanism of transition from a super-speed wave to a minimum speed wave. Another interesting phenomenon about the relation between the steady state wave speed and the behavior of the solution at infinity

*Corresponding author. *E-mail address*: asahinhc@gmail.com

IJNS.2014.06.15/808

was discovered by Larson[9] and Hagan[11]. They showed that for any initial condition of Fisher's equation such that $u_0(x) \sim e^{-\beta x}$ as $x \to \infty$, $u(x,t)$ evolves to a wave front as $t \to \infty$ with speed $c(\beta)$ given by

$$c(\beta) = \begin{cases} \beta + \dfrac{1}{\beta}, & \beta \leq 1, \\ 2, & \beta \geq 1. \end{cases}$$

Since the accurate representation of the travelling wave solution to Fisher's equation is a challenging numerical problem, many researchers paid attention to solve it numerically. Numerous computational methods including finite differences [12, 14, 16], finite elements [10, 13, 15], as well as the others [18, 19, 21, 23–25, 29] have been performed for the solution of Fisher's equation in the past. More recently, several B-spline finite element methods have also been presented for the numerical solution of Fisher's equation [26–28, 30].

The objective of the present study is to explore the viability of quintic B-spline collocation method for the numerical solution of the Fisher's equation. Our second objective is to make a comparison between the present method and some earlier studies.

This paper is organized as follows. Section 2 is devoted to description of both B-splines and collocation method. Von Neumann stability analysis is also given in this section. In section 3, numerical experiments are carried out to compare the accuracy, stability, flexibility, and efficiency of the scheme. Both the analytical solution and the steady state wave speed are used for a validation of the present approach. Conclusions are presented in section 4.

2 Numerical Method

We investigate the solution of Fisher's equation via the quintic B-spline collocation method. To construct the numerical method, we first need to generate a mesh. For this purpose, we consider the uniform mesh

$$a = x_0 < x_1 < \cdots < x_{N-1} < x_N = b$$

where $h = x_{m+1} - x_m$, $x_m = a + mh$, $m = 0, 1, ..., N$.

2.1 B-spline bases

One of the most known function class in mathematics is spline functions that have extensive application area in numerical analysis. The first mathematical reference to splines is the early work of Schoenberg[3] who revealed that splines have powerful approximation properties. Subsequently, many approximation methods have been employed [4].

A spline function is a sufficiently smooth piecewise polynomial of order k. It possesses a high degree of smoothness at the knots. A spline $S(x)$ of order k can be described in its B-representation

$$S(x) = \left\{ \sum_{m=1} \xi_m B_m^k(x) : \xi_m \text{ real, all } m \right\}$$

where $B_m^k(x)$ is a special spline function of order k called a B-spline which consists of polynomial pieces of **degree**$<k$.

B-spline functions play an important role in approximation and geometric modeling. They are used in data fitting, computer-aided design, automated manufacturing and computer graphics. In particular, after de Boor's [8] results about B-splines, spline techniques became popular for a broad range of applications [22]. Most properties and an efficient construction of B-splines can be found in [8]. Due to their some attractive properties such as having compact support and yielding numerical schemes with a high resolving power, B-splines are also widely used in differential problems. Because of having compact support, using B-splines in numerical solution of differential equations leads to sparse matrix systems.

The approximation of differential problems with B-splines is obtained by the method of weighted residual, of which the Galerkin and collocation methods are particular cases. The Galerkin method is the most widely used method for B-spline approximations on the other hand, the collocation method represents an economical alternative since it only requires the evaluation at grid points [20].

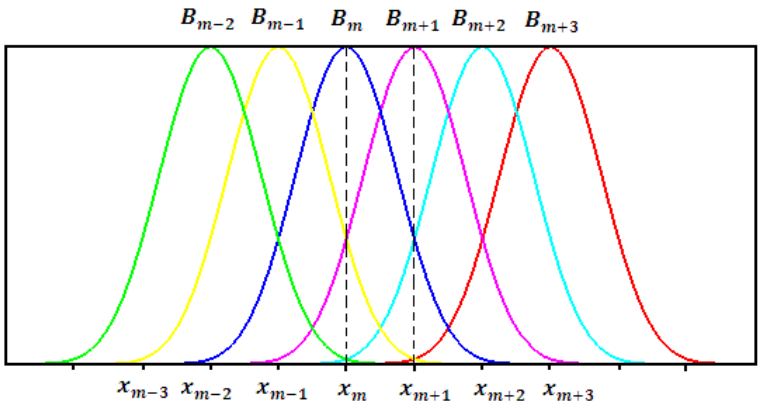

Figure 1: Quintic B-spline functions on a uniform mesh

Quintic B-splines are piecewise polynomials of degree five. Their mathematical expression can be given by

$$B_m(x) = \frac{1}{h^5}\begin{cases} (x-x_{m-3})^5, & [x_{m-3}, x_{m-2}] \\ (x-x_{m-3})^5 - 6(x-x_{m-2})^5, & [x_{m-2}, x_{m-1}] \\ (x-x_{m-3})^5 - 6(x-x_{m-2})^5 + 15(x-x_{m-1})^5, & [x_{m-1}, x_m] \\ (x-x_{m-3})^5 - 6(x-x_{m-2})^5 + 15(x-x_{m-1})^5 - 20(x-x_m)^5, & [x_m, x_{m+1}] \\ (x-x_{m-3})^5 - 6(x-x_{m-2})^5 + 15(x-x_{m-1})^5 - 20(x-x_m)^5 & \\ \qquad + 15(x-x_{m+1})^5, & [x_{m+1}, x_{m+2}] \\ (x-x_{m-3})^5 - 6(x-x_{m-2})^5 + 15(x-x_{m-1})^5 - 20(x-x_m)^5 & \\ \qquad + 15(x-x_{m+1})^5 - 6(x-x_{m+2})^5, & [x_{m+2}, x_{m+3}] \\ 0, & \text{otherwise} \end{cases}$$

Illustration of six successive quintic B-spline is presented in Fig.1. As shown in this figure, each quintic B-spline is non-zero over six adjacent elements so that six quintic B-splines cover each finite element.

2.2 Collocation method

The set of quintic B-splines $\{B_{-2}, B_{-1}, B_{-0}, ..., B_{N+2}\}$ forms a basis [7] for the functions defined over the solution domain. Hence the global approximation $U(x,t)$ to the function $u(x,t)$ can be formulated as

$$U(x,t) = \sum_{m=-2}^{N+2} \delta_m(t)\, B_m(x)$$

where δ_m are time dependent parameters which must be determined from the boundary and weighted residual conditions.

Over a standard element $[x_m, x_{m+1}]$, the trial function for U is written by

$$U(x,t) = \sum_{i=m-2}^{m+3} \delta_i(t)\, B_i(x)$$

where the quintic B-splines $B^e = \left\{B^5_{m-2}, B^5_{m-1}, B^5_m, B^5_{m+1}, B^5_{m+2}, B^5_{m+3}\right\}$ are only the B-splines non-zero over this finite element. Hence the nodal values and their derivatives are obtained in terms of δ_m by

$$\left.\begin{array}{lll} U(x_m) = U_m & = \delta_{m-2} + 26\delta_{m-1} + 66\delta_m + 26\delta_{m+1} + \delta_{m+2}, \\ U'(x_m) = U'_m & = \frac{5}{h}(\delta_{m+2} + 10\delta_{m+1} - 10\delta_{m-1} - \delta_{m-2}), \\ U''(x_m) = U''_m & = \frac{20}{h^2}(\delta_{m+2} + 2\delta_{m+1} - 6\delta_m + 2\delta_{m-1} + \delta_{m-2}), \\ U'''(x_m) = U'''_m & = \frac{60}{h^3}(\delta_{m+2} - 2\delta_{m+1} + 2\delta_{m-1} - \delta_{m-2}), \\ U''''(x_m) = U''''_m & = \frac{120}{h^4}(\delta_{m+2} - 4\delta_{m+1} + 6\delta_m - 4\delta_{m-1} + \delta_{m-2}). \end{array}\right\} \quad (5)$$

The collocation method where the weighting function is chosen as the dirac delta function in the finite element formulation of the problem consists in simply satisfying the equations at a discrete set of points $\{x_j,\ j=0,1,...,N\}$, the collocation points. With this choice, application of the numerical method turns into a substitution of nodal values U_m and their related derivatives into the Fisher's equation. In this point of view, Eq.(1) can be rewritten as follows:

$$\begin{aligned}\overset{\bullet}{\delta}_{m-2}+26\overset{\bullet}{\delta}_{m-1}+66\overset{\bullet}{\delta}_{m}+26\overset{\bullet}{\delta}_{m+1}+\overset{\bullet}{\delta}_{m+2} &= \frac{20\mu}{h^2}(\delta_{m+2}+2\delta_{m+1}-6\delta_m+2\delta_{m-1}+\delta_{m-2}) \\ &\quad +\rho z_m\left(\delta_{m-2}+26\delta_{m-1}+66\delta_m+26\delta_{m+1}+\delta_{m+2}\right),\end{aligned} \tag{6}$$

where $m=0,1,...,N$, $z_m=1-u_m$ and the notation $\bullet$ shows the derivative with respect to time.

Time discretization of Eq.(6) can be made with Crank-Nicolson formulas:

$$\overset{\bullet}{\delta}_m=\frac{\delta_m^{n+1}-\delta_m^n}{\Delta t},\quad \delta_m=\frac{\delta_m^{n+1}+\delta_m^n}{2}.$$

Using of above discretization formulas with some simple calculations the space discretized system (6) is rearranged as

$$\gamma_{m1}\delta_{m-2}^{n+1}+\gamma_{m2}\delta_{m-1}^{n+1}+\gamma_{m3}\delta_m^{n+1}+\gamma_{m2}\delta_{m+1}^{n+1}+\gamma_{m1}\delta_{m+2}^{n+1}=\gamma_{m4}\delta_{m-2}^{n}+\gamma_{m5}\delta_{m-1}^{n}+\gamma_{m6}\delta_m^{n}+\gamma_{m5}\delta_{m+1}^{n}+\gamma_{m4}\delta_{m+2}^{n} \tag{7}$$

where

$$\begin{aligned}&\gamma_{m1}=\frac{1}{\Delta t}-\frac{10\mu}{h^2}-\frac{\rho z_m}{2},\gamma_{m2}=\frac{26}{\Delta t}-\frac{20\mu}{h^2}-13\rho z_m,\gamma_{m3}=\frac{66}{\Delta t}+\frac{60\mu}{h^2}-33\rho z_m,\\ &\gamma_{m4}=\frac{1}{\Delta t}+\frac{10\mu}{h^2}+\frac{\rho z_m}{2},\ \gamma_{m5}=\frac{26}{\Delta t}+\frac{20\mu}{h^2}+13\rho z_m,\gamma_{m6}=\frac{66}{\Delta t}-\frac{60\mu}{h^2}+33\rho z_m.\end{aligned}$$

and the factor $(1-u)$ in nonlinear term of Eq.(1) is considered as locally constant, i.e. $z_m=1-U_m^n$.

There are $N+1$ equations but $N+5$ unknown parameters in system (7). To solve this system the number of equations and the number of unknown parameters must be equalized. Using the boundary conditions enables us to eliminate the boundary parameters δ_{-2}^{n+1}, δ_{-1}^{n+1} and δ_{N+1}^{n+1}, δ_{N+2}^{n+1} from the system (7) so that we obtain a solvable penta-diagonal band matrix system that can be solved by the Thomas algorithm. In order to start the iteration, computation of the initial parameters δ_m^0 is needed. Once the initial parameters are determined, time evolutions of δ_m^n are found from the recurrence relationship (7). The initial condition of the problem and the Eqs.(5) are used for this purpose.

In computation of the nonlinear term, an inner iteration

$$(\delta^*)_m^{n+1}=\delta_m^n+\frac{1}{2}\left(\delta_m^{n+1}-\delta_m^n\right),\quad m=0,1,...,N$$

may be used two or three times in each time step to make the solution parameters better.

2.2.1 Stability

Von Neumann stability analysis is an extremely useful method for understanding the propagation of errors in linear difference equations. By considering a general term in the closed form Fourier series solution of the discrete system, one can examine the potential for amplification of any of the possible Fourier modes which are sustainable on a discrete mesh.

In this analysis, the solution at point (x_{m+1},t_{n+1}) can be related to that at point (x_m,t_n) through the relationship

$$u_{m+1}^{n+1}=qe^{ikh}u_m^n$$

where i in the exponential is $\sqrt{-1}$ and kh is the dimensionless wave numbers. Stability analysis in this context then amounts to ensuring $|q|\leq 1$ over all possible values of kh ranging between 0 (infinite wavelength) and π (shortest wavelength on a discrete mesh) [17].

After the substitution of the Fourier mode

$$\delta_m^n=q^ne^{imkh}$$

in difference equation (7) we obtain the growth factor q as

$$q=\frac{2\gamma_{m4}\cos(2kh)+2\gamma_{m5}\cos(kh)+\gamma_{m6}}{2\gamma_{m1}\cos(2kh)+2\gamma_{m2}\cos(kh)+\gamma_{m3}}$$

The stability condition $|q| \leq 1$ leads to the following results:

$$\begin{aligned} |q| \leq 1 \quad &\Rightarrow |q|^2 \leq 1 \\ &\Rightarrow \left(2\gamma_{m4}\cos(2kh) + 2\gamma_{m5}\cos(kh) + \gamma_{m6}\right)^2 - \left(2\gamma_{m1}\cos(2kh) + 2\gamma_{m2}\cos(kh) + \gamma_{m3}\right)^2 \leq 0 \\ &\Rightarrow \frac{32AB}{\Delta t h^2} \leq 0 \end{aligned}$$

where

$$\begin{aligned} A &= \cos^2(kh) + 13\cos(kh) + 16 \\ B &= 20\mu\cos^2(kh) + \rho z_m h^2 \cos^2(kh) + 20\mu\cos(kh) + 13\rho z_m h^2 \cos(kh) - 40\mu + 16\rho z_m h^2 \end{aligned}$$

Since the all other terms are strictly positive, the only condition for the stability comes from the term B which must be less than or equal to zero. After some operations the mentioned necessity gives the condition

$$\frac{\mu}{\rho z_m h^2} \leq \frac{16 + 13\cos(kh) + \cos^2(kh)}{20\left(2 - \cos(kh) - \cos^2(kh)\right)} \tag{8}$$

Hence the numerical method is conditionally stable with condition (8).

Since $\cos(kh)$ varies in $[-1, 1]$ and both left and right hand side terms tend to infinity when $h \to 0$, it is not seem easy to make this condition simpler for h value. However, it can be said from the condition that stability of the method does not depend on time stepping, i.e. the numerical method is unconditionally stable in terms of time step Δt. So, in numerical computations, we will choose h value empirically after fixing the time step Δt.

3 Numerical Experiments

In this section, we examine the performance of the proposed numerical method. First, we consider an initial pulse disturbance to demonstrate the reaction and the diffusion processes in the solution domain. Similar observation with an initial step disturbance is presented as a second test problem. A second-order perturbation solution is also studied in the next subsection. Finally, to make a detailed comparison between the present method and some other methods from the literature, we validate our method on the weak reaction and the strong reaction problem.

To analyze the numerical performance of the given method, we use two error measurements, that is, the maximum absolute error L_∞ and L_2 error norm which are defined by

$$L_\infty = \left\|u^{exact} - u^{numeric}\right\|_\infty = \max_j \left|u_j^{exact} - u_j^{numeric}\right|,$$

$$L_2 = \left\|u^{exact} - u^{numeric}\right\|_2 = \sqrt{h\sum_{j=0}^{N}\left(u_j^{exact} - u_j^{numeric}\right)^2}.$$

The difference of the theoretical and the numerical wave speeds $|c - \hat{c}|$ can also be used as an approximation for the error when the solution reaches the steady state motion. In order to calculate the speed of the simulated traveling wave solution, we use the formula appeared in [15]

$$c^n = \frac{\left(x_{wf}^n - x_{wf}^{n-1}\right)}{\Delta t} \tag{9}$$

where

$$x_{wf}^n = \int_0^L u(x, t_n)\, dx \Big/ \max_{0 \leq x \leq L}\{u(x, t_n)\}$$

is a reference position for the propagating wave-front. Then the transformed wave speed c_s is computed by $c_s = c \big/ \sqrt{\mu\rho}$. The above integral is approximated by using the trapezoid rule.

To compute the pointwise rate of convergence, the algorithm has been run for various space steps. The order of the convergence for the method is calculated by the formula

$$\textbf{order} = \frac{\log(\|u - u_{h_i}\|_2 \,/\, \|u - u_{h_{i+1}}\|_2)}{\log(h_i/h_{i+1})}$$

where u is the exact solution and u_{h_i} is the numerical solution with step size h_i.

3.1 Initial pulse profile

To see the effects of reaction and diffusion, we consider the pulse disturbance

$$u(x,0) = sech^2(10x), \quad x \in (-\infty, \infty) \tag{10}$$

as the initial condition of Eq.(1) with the boundary conditions (4).

Since initial disturbance (10) and the results obtained from that are almost zero after some x points, we can choose the interval $[-50, 50]$ as a solution domain for the programming purpose. So, the local boundary conditions (4) turn into the following artificial form for this restricted domain:

$$u(-50,t) = u(50,t) = 0, \quad t > 0.$$

In computation, the coefficients in Eq.(1) are taken as $\mu = 0.1$ and $\rho = 1$ with the discretization parameters $h = 0.025$ and $\Delta t = 0.05$.

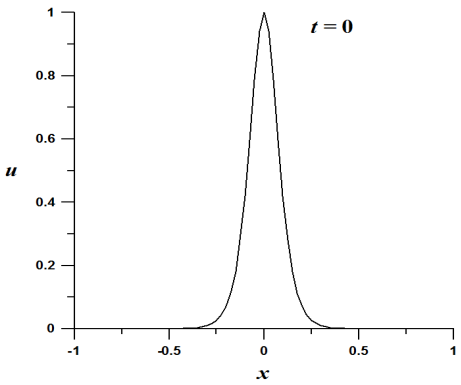

Figure 2: Initial solution

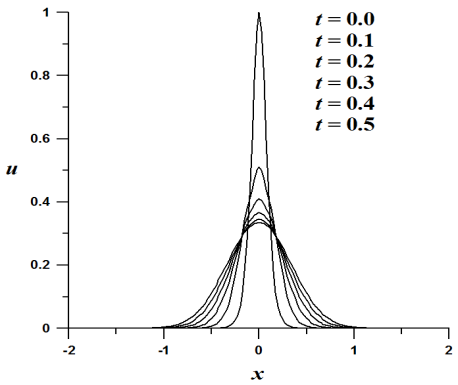

Figure 3: Solutions at early times

As seen clearly from Figs.2 and 3, initially, the diffusion term u_{xx} is negative and it has a large absolute value however the reaction term $u(1-u)$ is very small. So the effect of diffusion dominates over the effect of reaction and the peak initially goes down rapidly and then becomes flatter. When the peak takes its minimum value, the reaction term starts to dominate the diffusion term slowly so that the peak increases and the amplitude grows as indicated in Fig.4. After the peak reached the maximum value $u = 1$, the top of the graph becomes flatter and flatter. This behavior is illustrated in Fig.5.

Population density profile with respect to time is an another useful tool for understanding the reaction and diffusion process at some specified positions. Fig.6 shows how the population density changes at distinct points $x = 0$, 1, 10, 20. As expected from the above discussion, there is no decay in population without the origin between these points. The decrement in population density at the origin continues until the time $t = 0.65$ with the maximum decay almost 67%, then it starts to increase and arrives the highest level.

The difference of the theoretical and the numerical wave speeds can be used to measure the accuracy of the method in this problem. Depending on the selection of $\mu = 0.1$ and $\rho = 1$ the steady-state value for the theoretical speed is $2\sqrt{\mu\rho} = 0.63246$. Similar to the results of [13, 15] the wave speed c approaches the steady-state value while the transformed wave speed $\hat{c}_s$ approaches the minimum speed $c_{s_{\min}} = 2$. In order to observe the mentioned approach, numerical wave speeds are depicted in Fig.7. Additionally, to give a comparison, the wave speeds and the related errors are tabulated in Table 1 for $t = 40$. The calculated numerical wave speeds are in good agreement with the theoretical results and some earlier studies from the literature.

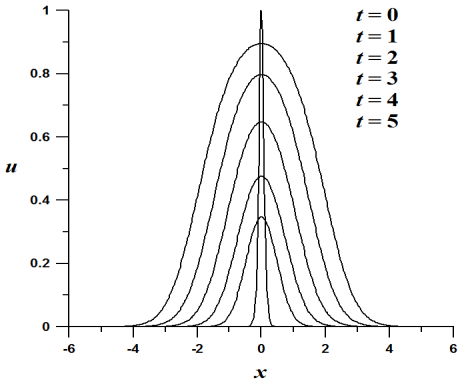

Figure 4: Short time behavior

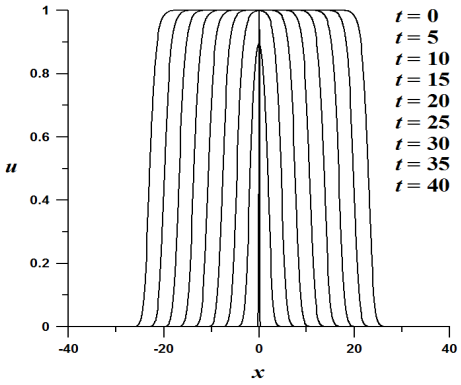

Figure 5: Long time behavior

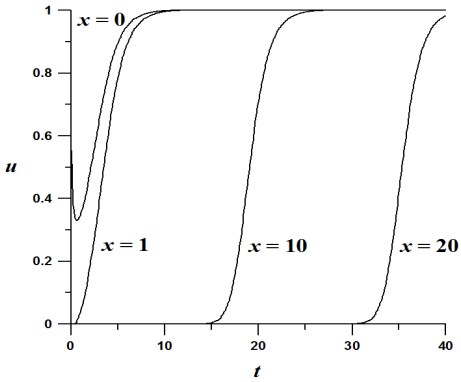

Figure 6: Changes at population

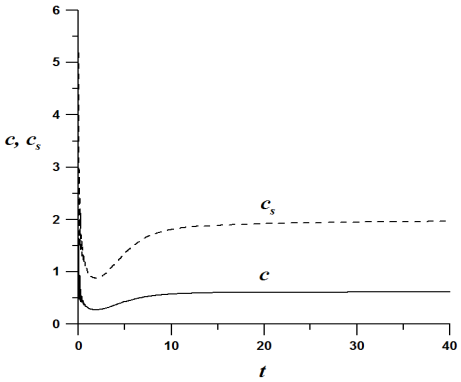

Figure 7: Changes at wave speed

Table 1: Comparison of the wave speeds and errors at $t = 40$

	Speeds		Errors	
	$\hat{c}$	$\hat{c}_s$	$\lvert c - \hat{c}\rvert$	$\lvert c_s - \hat{c}_s\rvert$
Present	0.6214	1.9650	0.0111	0.0350
[27]	0.6214	1.9651	0.0111	0.0349
[15]	0.6210	1.9638	0.0115	0.0362
[13]	0.6205		0.0120	
Exact	0.6325	2.0000		

3.2 Initial step profile

By considering the step disturbance

$$u(x,0) = \begin{cases} e^{10(x+1)}, & x < -1 \\ 1, & -1 \le x \le 1 \\ e^{-10(x-1)}, & x > 1 \end{cases} \tag{11}$$

as an initial condition for Eq. (1), similar with previous problem, we observe reaction and diffusion process in this experiment where the boundary conditions and the solution parameters are chosen as same with in the first test problem.

The initial profile of the solution is given in Fig.8. Different from previous one, effects of diffusion and reaction are very small in this case. As seen in Fig.9, diffusion is more effective than reaction near the corners so that the effects of diffusion at the edges change the graph from having sharp points to being smooth and cause a going down a little bit (see Fig.10), then the top of the wave comes up and becomes flatter and flatter in long time period which is illustrated in Fig.11.

Population density-time graphs at distinct points $x = 0,\ 1,\ 10,\ 20$ are given in Fig.12. Although there is a decay in population at the origin (the decay is only 2%), the only remarkable decrement between these positions is at $x = 1$ where the maximum decay is about 32% at time $t = 0.45$. Since diffusion is more effective at $x = 1$, this result is due.

Since we use the parameters same with the first problem, the steady-state value of the speed and the minimum value for the transformed wave speed are 0.63246 and 2 respectively. Fig.13 shows that numerical wave speeds approach these values.

Wave speed comparison is presented in Table 2 for this problem. According to Table 2 obtained results are acceptable and in unison with the other given results.

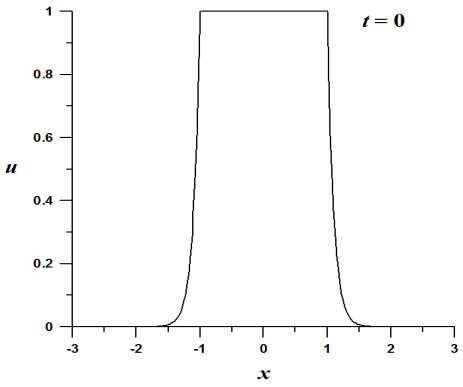

Figure 8: Initial solution

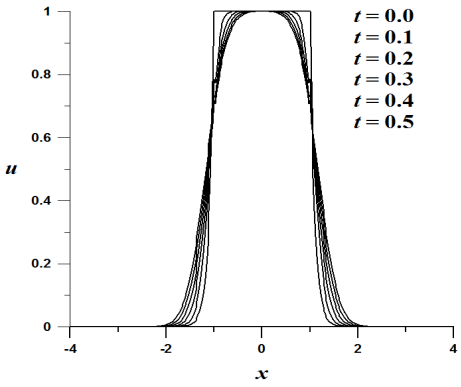

Figure 9: Solutions at early times

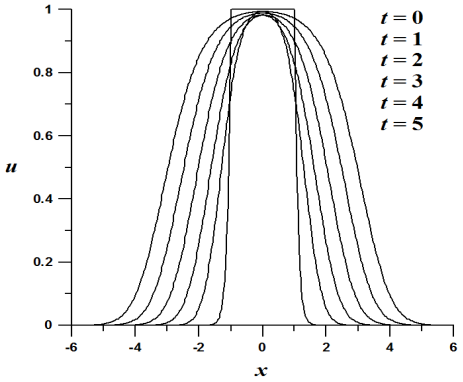

Figure 10: Short time behavior

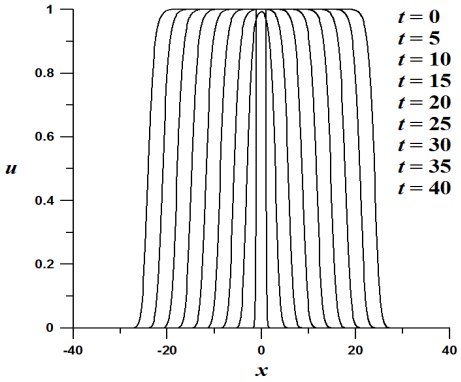

Figure 11: Long time behavior

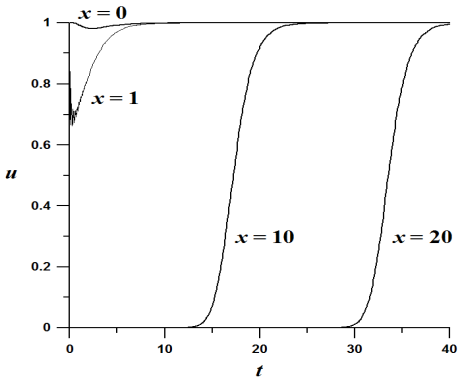

Figure 12: Changes at population

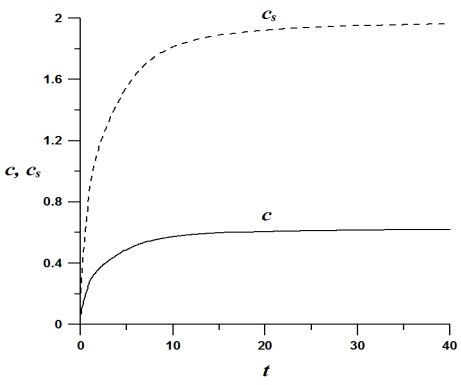

Figure 13: Changes at wave speeds

Table 2: Comparison of the wave speeds and errors at $t = 40$

	Speeds		Errors	
	$\hat{c}$	$\hat{c}_s$	$\lvert c - \hat{c}\rvert$	$\lvert c_s - \hat{c}_s\rvert$
Present	0.6213	1.9648	0.0112	0.0352
[27]	0.6214	1.9649	0.0111	0.0351
[15]	0.6520	2.0620	0.0195	0.0620
Exact	0.6325	2.0000		

3.3 Super-speed wave front

Thirdly, a second-order perturbation solution given by Gazdag and Canosa[6] is studied. Here we consider the unscaled form of the problem for which the initial condition is given by

$$u(x,0) = \frac{1}{1+e^{\frac{\rho z}{c}}} - \frac{\mu\rho e^{\frac{\rho z}{c}}}{c^2(1+e^{\frac{\rho z}{c}})^2}\left[1 - \ln\frac{4e^{\frac{\rho z}{c}}}{(1+e^{\frac{\rho z}{c}})^2}\right]$$

where c denotes the actual wave speed, d is the original unscaled frame and $z = x - ct - d$. In this test problem, the initial profile is chosen symmetric about the origin and local boundary conditions (4) are used. More discussion about this problem can be found in [6], [15].

In computation, numerical parameters are taken as

$$\mu = \rho = 1,\ h = 0.5,\ \Delta t = 0.05,\ d = 40$$

and the solutions are obtained over the interval $[-500, 500]$.

The initial distribution is shown in Fig.14 for $c = 2$. This initial profile sometimes becomes negative. Although it is not seen in this figure, it causes unstable solutions in time period. To overcome this difficulty, similar to the approach of Carey and Shen[15], we force $u = 0$ where the initial profile is negative then solutions remain stable.

The wave profiles are depicted in Figs.15, 16 and 17 for the speed values 2, 4 and 6 respectively. As shown in Fig.15, when the speed value is 2, there is no change in the wave propagates. On the other hand, when the speed c takes the values 4 and 6, corresponding to super-speed waves, the wave propagations steepen and evolve gradually to a minimum speed wave.

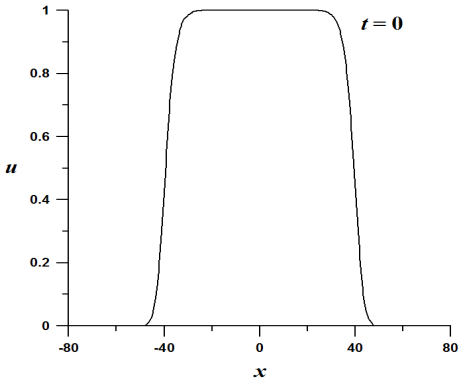

Figure 14: Initial solution for c = 2

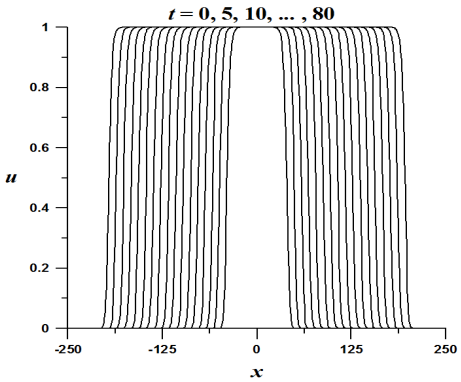

Figure 15: Solutions for c = 2

The obtained results are almost the same as the results obtained by Carey and Shen[15]. Although there are some small differences between the obtained results and those described by Gazdag and Canosa[6], our results are in a good agreement with their results. In comparison, the transition time in the present method and in the study of [15] from super speed wave to minimum speed wave is longer than in the work[6]. Besides, the mentioned transition in our study is smoother than the study of Gazdag and Canosa[6].

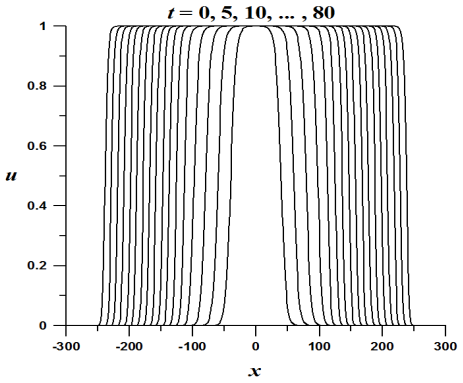

Figure 16: Solutions for c = 4

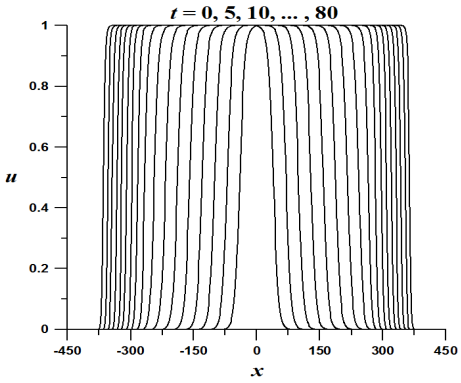

Figure 17: Solutions for c = 6

3.4 Strong reaction

Finally, we consider a modified form of Fisher Equation in which the diffusion term is much smaller than the reaction term

$$\frac{\partial u}{\partial t} = \frac{\partial^2 u}{\partial x^2} + \rho u(1-u), \quad -\infty < x < \infty,\ t > 0 \tag{12}$$

where ρ is a positive constant so that $\rho \gg 1$. A particular solution of this modified equation has a travelling wave solution of the form

$$u(x,t) = \left[1 + \exp\left(\sqrt{\frac{\rho}{6}}x - \frac{5\rho}{6}t\right)\right]^{-2} \tag{13}$$

which travels with constant speed $c = 5\sqrt{\rho/6}$ and satisfies the nonlocal conditions (2) and (3).

To make a comparison with the results of [23] and to see the rate of convergence, we first solved the problem with $\rho = 1$ that leads to wave speed $c = 5\sqrt{1/6} \approx 2.04124145 > 2$ before the strong reaction case. Table 3 shows the errors in detail with three different error norms. In comparison, the present method is more accurate than CN and ASD, on the other hand the results of FPS and DSC are better than the present. The orders for rate of convergence are tabulated in Table 4 which shows that the present method has second order temporal accuracy whereas its spatial order is different. Although the method gives high spatial orders for $h = 2$ and $h = 1$, it yields almost same errors for $h = 0.5$ and $h = 0.25$ and so the spatial order decreases.

Table 3: Comparison of short-term solution of a scaled Fisher's equation with $\rho = 1$

				$t = 5.0$			$t = 10.0$		
Scheme	N	h	Δt	L_∞	L_2	$\lvert c-\hat{c}\rvert$	L_∞	L_2	$\lvert c-\hat{c}\rvert$
Present	128	1.0	0.2	3.52e−3	7.60e−3	9.50e−3	1.11e−2	2.55e−2	1.50e−2
	128	1.0	0.1	8.80e−4	1.89e−3	2.39e−3	2.81e−3	6.45e−3	3.85e−3
	64	2.0	0.01	9.78e−5	2.46e−4	2.14e−4	8.82e−4	1.87e−3	2.25e−3
	128	1.0	0.01	5.65e−6	1.35e−5	3.11e−5	8.04e−5	1.76e−4	1.94e−4
[23] CN	512	1.0	0.2	5.18e−3	1.10e−3	1.18e−2	1.43e−2	2.99e−3	1.69e−2
	512	1.0	0.1	1.35e−3	2.91e−4	3.48e−3	4.25e−3	8.88e−4	5.53e−3
	64	2.0	0.01	1.02e−2	1.87e−3	4.47e−2	5.47e−2	1.16e−2	1.04e−1
	128	1.0	0.01	2.66e−3	4.84e−4	1.15e−3	1.46e−2	3.06e−3	2.77e−2
[23] ASD	128	1.0	0.2	3.84e−2	7.24e−3	9.38e−2	1.09e−1	2.19e−2	1.26e−1
	128	1.0	0.1	1.96e−2	3.73e−3	4.93e−2	5.62e−2	1.14e−2	6.68e−2
	64	2.0	0.01	1.99e−3	3.83e−4	5.16e−3	5.67e−3	1.18e−3	7.06e−3
	128	1.0	0.01	1.99e−3	3.83e−4	5.16e−3	5.72e−3	1.18e−3	7.06e−3
[23] FPS	128	1.0	0.2	1.34e−5	2.74e−6	4.25e−5	5.61e−5	1.17e−5	9.15e−5
	128	1.0	0.1	9.01e−7	1.84e−7	2.94e−6	3.86e−6	8.03e−7	6.41e−6
	64	2.0	0.01	3.16e−6	6.75e−7	6.89e−8	3.21e−6	6.76e−7	1.10e−7
	128	1.0	0.01	1.27e−9	1.38e−10	4.01e−9	4.40e−10	8.78e−11	7.58e−10
[23] DSC	128	1.0	0.2	1.34e−5	2.74e−6	4.25e−5	5.61e−5	1.17e−5	9.15e−5
	128	1.0	0.1	9.00e−7	1.84e−7	2.95e−6	3.86e−6	8.03e−7	6.41e−6
	64	2.0	0.01	4.35e−6	9.38e−7	1.34e−7	3.12e−6	6.50e−7	1.19e−7
	128	1.0	0.01	1.59e−9	2.50e−10	7.02e−9	1.39e−9	2.06e−10	8.43e−10

Table 4: Rate of convergence

Spatial order $(\Delta t = 0.01)$			Temporal order $(h = 1.0)$		
h_i	$t = 5$	$t = 10$	Δt_i	$t = 5$	$t = 10$
2.00			0.200		
1.00	4.18566	3.40724	0.100	2.00412	1.98237
0.50	−0.44913	1.32379	0.050	2.02090	1.92680
0.25	−0.04591	0.13910	0.025	2.08996	1.74021

We consider the strong reaction problem by choosing $\rho = 10^4$ in Eq.(12). Hence the wave speed of the analytical solution (13) is $c = 5\sqrt{10^4/6} \approx 204.124$. With the strong reaction force, the solution evolves into a shock-like wave. Therefore, to represent the rapidly changing solution correctly, very fine mesh has to be used in a low order method. Non-uniform mesh can be used to avoid the large computation cost. Li et al.[18] and Qiu and Sloan[19] considered this strong

reaction problem using moving mesh schemes. Olmos and Shizgal[25] solved this problem by using the overlapped multi domain approach. In this study, we consider a uniform mesh for the strong reaction problem. Discretization parameters are chosen as $N = 64$ and $\Delta t = 5 \times 10^{-6}$. The solution domain is taken as $[-0.2, 0.8]$. The numerical results and the analytical solution are illustrated together (continuous line is the analytical solution) in Fig.18 at times $t = 0$, 5×10^{-4}, 1×10^{-3}, 1.5×10^{-3}, ..., 3.5×10^{-3}. The error distributions at different times are graphed in Fig.19 where the error at the right hand boundary at $t = 0.0035$ can be reduced to zero by extending the solution domain at that boundary. To see the accuracy of the present method, the obtained results are tabulated in Table 5. In comparison, again the results of **DSC** and **FPS** [23] are better than the purposed method while the present is more accurate than the results of [27] and **CN**, **ASD** in [23] and almost same with the results of [19]

Table 5

Comparison of short-term solution of a scaled Fisher's equation with $\rho = 10^4$, $N = 64$, $\Delta t = 5.0\text{e}{-6}$. The results from [19] are (a) MMDAE with $N = 50$, (b) MMPDE6 with $N = 50$ and $\tau = 10^{-7}$ and (c) method of lines on an even spaced grid with $N = 300$.

		t						
Scheme	Error	5.00e−4	1.00e−3	1.50e−3	2.00e−3	2.50e−3	3.00e−3	3.50e−3
Present	L_∞	2.05e−4	9.81e−4	2.30e−3	3.90e−3	5.49e−3	7.42e−3	9.04e−3
	L_2	4.25e−5	2.25e−4	5.35e−4	9.08e−4	1.31e−3	1.74e−3	2.18e−3
	$\lvert c-\hat{c}\rvert$	6.14e−2	1.80e−1	2.44e−1	2.76e−1	2.93e−1	3.02e−1	1.98e−1
[27]	L_∞	2.55e−3		1.62e−1		8.65e−2		6.98e−2
	L_2	6.47e−4		3.80e−1		2.03e−2		1.59e−2
	$\lvert c-\hat{c}\rvert$	1.85e+0		5.58e+0		1.12e+1		1.26e+1
[23] CN	L_∞	1.03e−2	5.55e−2	1.25e−1	2.04e−1	2.80e−1	3.60e−1	4.48e−1
	L_2	1.92e−3	1.17e−2	2.65e−2	4.36e−2	6.18e−2	8.04e−2	9.91e−2
	$\lvert c-\hat{c}\rvert$	4.49e+0	1.04e+1	1.31e+1	1.46e+1	1.54e+1	1.60e+1	1.64e+1
[23] ASD	L_∞	1.07e−2	2.88e−2	4.93e−2	7.10e−2	9.37e−2	1.24e−1	9.44e−1
	L_2	2.09e−3	6.07e−3	1.06e−2	1.53e−2	2.02e−2	2.68e−2	2.35e−1
	$\lvert c-\hat{c}\rvert$	2.61e+0	3.45e+0	3.70e+0	3.80e+0	4.05e+0	1.59e+1	3.41e+2
[23] FPS	L_∞	3.13E−6	3.47e−6	3.90e−6	5.00e−6	7.82e−5	4.23e−3	3.42e−1
	L_2	7.71E−7	6.79e−7	7.02e−7	9.04e−7	2.11e−5	1.19e−3	8.95e−2
	$\lvert c-\hat{c}\rvert$	1.58E−3	7.72e−5	9.73e−5	1.87e−3	9.68e−2	5.54e−0	4.76e+2
[23] DSC	L_∞	6.28E−6	3.03e−6	1.98e−6	3.23e−6	4.46e−6	5.44e−6	6.22e−6
	L_2	1.24E−6	6.53e−7	5.92e−7	8.35e−7	1.16e−6	1.43e−6	1.64e−6
	$\lvert c-\hat{c}\rvert$	2.53E−3	1.06e−4	6.23e−5	6.58e−5	7.37e−5	1.00e−4	5.19e−4
[19] (a)	L_∞					9.25e−3		
(b)	L_∞					4.29e−2		
(c)	L_∞					9.34e−3		

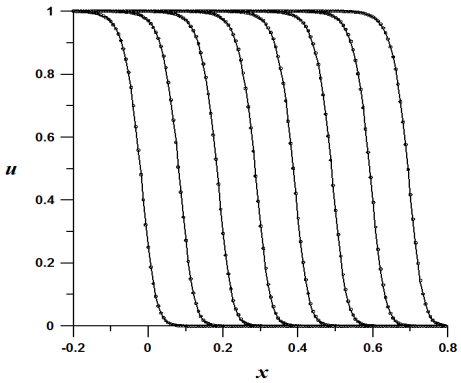

Figure 18: Solution profiles

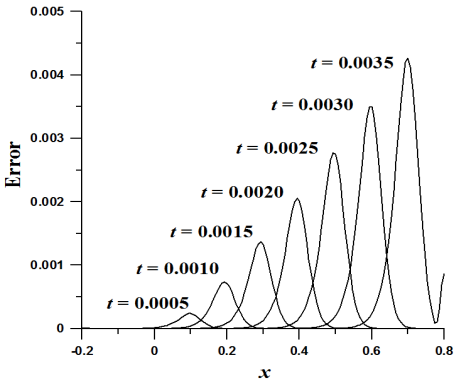

Figure 19: Absolute error distributions

4 Conclusions

This study explores the utility of quintic B-spline collocation method in the solution of Fisher's equation. Forward difference and Crank-Nicolson formulas are used for time discretization of the equation. To investigate the stability of the method we employed the Von Neumann stability analysis. Four numerical experiments considered to illustrate the accuracy and the efficiency of the present method. Numerical results are compared with analytical solutions or the steady state wave speed. Obtained results are acceptable in terms of accuracy. Temporal order of convergence shows that the present method has second order accuracy.

The main advantage of the presented method is the yielding less computational cost in the solution process. The method leads to a matrix equation where the coefficient matrix is 5-band matrix and it requires relatively less CPU time. Also simplicity in the implementation process of the collocation method can be stated as an another advantage.

In conclusion, quintic B-spline collocation method simulates the solution profiles successfully and it yields acceptable results in comparison. In terms of accuracy, flexibility, stability, and efficiency it is comparable with other existing numerical methods for the solution of Fisher's equation

Acknowledgments

The first author thanks to Council of Higher Education of Turkey for their financial support during his research program.

References

[1] R.A.Fisher, The wave of advance of advantageous genes, *Ann. Eugen* , 7(1936):355-369.

[2] A.Kolmogorov, I.Petrovsky and N.Piscounoff, Study of the diffusion equation with growth of the quantity of matter and its application to biology problems, *Bulletin de l'université d'état à Moscou, Ser. int., Section A*, 1(1937):1-25.

[3] I.J.Schoenberg, Contributions to the problem of approximation of equidistant data by analytic functions, *Quart. Appl. Math.*, 4(1946):45-99 and 112-141.

[4] J.H.Ahlberg, E.N.Nielson and J.L.Walsh, TheTheory of Splines and Their Applications, Academic Press, New York. 1967.

[5] J.Canosa, On a nonlinear diffusion equation describing population growth, *IBM J. Res. Develop.*, 17(1973):307-313.

[6] J.Gazdag and J.Canosa, Numerical solution of Fisher's equation, *J. Appl. Prob.*, 11(1974):445-457.

[7] P.M.Prenter, Splines and variational methods, J.Wiley, New York. 1975.

[8] C. de Boor, A Practical Guide to Splines, Springer. 1978.

[9] D.A.Larson, Transient bounds and time asymptotic behavior of solutions to nonlinear equations of Fisher type, *SIAM J. Appl. Math.*, 34(1978):93-103.

[10] A.R.Mitchell and V.S.Manoranjan, Finite element studies of reaction-diffusion. pp 17-36 of J.R.Whitehad (Ed.), The Mathematics of Finite Elements and Applications, Academic Press, London. 1981.

[11] P.Hagan, Travelling wave and multiple travelling wave solutions of parabolic equations, *SIAM J. Math. Anal.*, 13(1982):717-738.

[12] T. Hagstrom and H. B. Keller, The numerical calculation of traveling wave solutions of non-linear parabolic equations, *SIAM J. Sci. and Stat. Comput*, 7(3)(1986):978-988.

[13] S.Tang and R.O.Weber, Numerical study of Fisher's equation by a Petrov-Galerkin finite element method, *J. Austral. Math. Soc. Ser. B*, 33(1991):27-38.

[14] R. E. Mickens, A best finite-difference scheme for the Fisher equation, *Numer. Methods Partial Differential Eq.*, 10(1994):581-585.

[15] G.F.Carey and Yun Shen, Least-Squares finite element approximation of Fisher's reaction-diffusion equation, *Numer. Methods Partial Differential Eq.*, 11(1995):175-186.

[16] R. E. Mickens, Relation between the time and space step-sizes in nonstandard finite-difference schemes for the Fisher equation, *Numer. Methods Partial Differential Eq.*, 13(1997):51-55.

[17] Michael I. Miga, Keith D. Paulsen and Francis E. Kennedy, Von Neumann stability analysis of Biot's general two-dimensional theory of consolidation, *Int. J. Numer. Meth. Engng.*, 43(1998):955-974.

[18] S.Li, L.R.Petzold and Y.Ren, Stability of moving mesh systems of partial differential equations, *SIAM J. Sci. Comput.*, 20(1998):719-738.

[19] Y.Qiu and D.M.Sloan, Numerical solution of Fisher's equation using a moving mesh method, *J. Comput. Phys.*, 146(1998):726-746.

[20] O.Botella, A velocity-pressure Navier-Stokes solver using a B-spline collocation method, Center for Turbulence Research-Annual Research Briefs. 1999.

[21] K.Al-Khaled, Numerical study of Fisher's reaction-diffusion equation by the Sinc collocation method, *J. Comput. Appl. Math.*, 137(2001):245-255.

[22] K.Höllig, Finite Element Methods with B-Splines, The SIAM series on Frontiers in Applied Mathematics. 2003.

[23] S.Zhao and G.W.Wei, Comparison of the discrete singular convolution and three other numerical schemes for solving Fisher's equation, *SIAM J. Sci. Comput.*, 25(2003):127-147.

[24] J.I.Ramos, Exponential methods for one-dimensional reaction–diffusion equations, *Applied Mathematics and Computation*, 170(2005):380-398.

[25] D.Olmos and B.D.Shizgal, A pseudospectral method of solution of Fisher's equation, *J. Comput. Appl. Math.*, 193(2006):219-242.

[26] A.Şahin, İ.Dağ and B.Saka, A B-spline algorithm for the numerical solution of Fisher's equation, *Kybernetes*, 37(2)(2008):326-342.

[27] İ.Dağ, A.Şahin and A.Korkmaz, Numerical investigation of the solution of Fisher's equation via the B-spline Galerkin method, *Numer. Methods Partial Differential Eq.*, 26(2010):1483-1503.

[28] R.C.Mittal and G.Arora, Efficient numerical solution of Fisher's equation by using B-spline method, *International Journal of Computer Mathematics*, 87(13)(2010):3039-3051.

[29] M.Bastani and D.K.Salkuyeh, A highly accurate method to solve Fisher's equation, *Pramana-Journal of Physics*, 78(3)(2012):335-346.

[30] R.C.Mittal and R.K.Jain, Numerical solutions of nonlinear Fisher's reaction–diffusion equation with modified cubic B-spline collocation method, *Mathematical Sciences*,7:12(2013).